Translational Oncology 27 (2023) 101569

Contents lists available at ScienceDirect

Translational Oncology

journal homepage: www.elsevier.com/locate/tranon

Telomerase inhibitor MST-312 and quercetin synergistically inhibit cancer cell proliferation by promoting DNA damage

Stina George Fernandes [1], Kavita Gala [1], Ekta Khattar [*]

Sunandan Divatia School of Science, Biological Sciences, Narsee Monjee Institute of Management Studies University, SVKM's NMIMS (Deemed to be University), Room 747, Mithibhai Building, VL Mehta Marg Vile Parle West, Vile Parle West, Mumbai, Maharashtra 400056, India

ARTICLE INFO

Keywords:
Telomerase inhibitor MST-312
Quercetin
Cancer
DNA damage response
Synergism

ABSTRACT

Quercetin is a natural flavonoid with well-established anti-proliferative activities against a variety of cancers. Telomerase inhibitor MST-312 also exhibits anti-proliferative effect on various cancer cells independent of its effect on telomere shortening. However, due to their low absorption and toxicity at higher doses, their clinical development is limited. In the present study, we examine the synergistic potential of their combination in cancer cells, which may result in a decrease in the therapeutic dosage of these compounds. We report that MST-312 and quercetin exhibit strong synergism in ovarian cancer cells with combination index range from 0.2 to 0.7. Co-treatment with MST-312 and quercetin upregulates the DNA damage and augments apoptosis when compared to treatment with either compound alone or a vehicle. We also examined the effect of these compounds on the proliferation of normal ovarian surface epithelial cells (OSEs). MST-312 has a cytoprotective impact in OSEs at lower dosages, but is inhibitory at higher doses. Quercetin did not affect the OSEs proliferation at low concentrations while at higher concentrations it is inhibitory. Notably, combination of MST-312 and quercetin had no discernible impact on OSEs. These observations have significant implications for future efforts towards maximizing efficacy in cancer therapeutics as this co-treatment specifically affects cancer cells and reduces the effective dosage of both the compounds.

Introduction

Ovarian cancer is the seventh most common type of cancer in women [1]. According to a study published in 2020, more than three lakh cases of ovarian cancer occurred worldwide, with the majority of women presenting with advanced disease, chemotherapeutic drug resistance, and relapse [2,3]. Hence, there is a need to develop newer, sustainable strategies to target the disease.

Numerous plant-derived compounds exhibit anticancer properties as they possess high therapeutic potential and display low cytotoxicity towards healthy tissues [4]. One such phytochemical is quercetin (2-(3, 4-dihy-droxyphenyl)-3,5,7-trihydroxy4H-chromen-4-one), a polyphenolic flavonoid present in common fruits and vegetables like apples, red grapes, raspberries, cherries, onions, tomatoes, broccoli, kale, etc. [5]. Due to the presence of two critical pharmacophores i.e. a catechol group and an OH-group, quercetin functions as an ideal antioxidant to scavenge free radicals [6]. Quercetin also exhibits anticancer activity in different human cancers such as breast, colon, kidney, liver, lung, prostate, pancreatic, skin as well as in ovarian cancers among others [7, 8]. Suggested mechanism of action includes its anti-oxidative activity, interaction with various cellular receptors and modulation of important signal transduction pathways (for example cell cycle regulation, proliferation, apoptosis and inflammation) [8,9]. Quercetin exhibits reduced cytotoxicity towards normal cells and its co-treatment with several chemotherapeutic drugs and compounds augments anticancer treatment strategies [10–14].

MST-312 is a chemical derivative of epigallocatechin gallate (EGCG), the primary catechin present in green tea. MST-312 is more stable and potent at causing growth arrest in cancer cells than EGCG [15]. MST-312 inhibits telomerase activity in tumor cells and induces growth arrest and apoptosis via induction of telomeric DNA damage, activation of DNA damage response and inhibition of the NF-κB pathway [15–18].

Combination treatment with quercetin and EGCG has additive anticancer effect on prostate cancer cells [19,20]. The additive effect is due to their combined action on catechol-O-methyl transferase (COMT) activity and protein expression levels. COMT is involved in the

* Corresponding author.
E-mail address: Ekta.Khattar@nmims.edu (E. Khattar).
[1] These authors contributed equal to this work.

https://doi.org/10.1016/j.tranon.2022.101569
Received 25 February 2022; Received in revised form 29 September 2022; Accepted 14 October 2022

methylation of green tea polyphenols resulting in their inactivation and since quercetin reduces the protein expression of COMT, co-treatment of quercetin with EGCG showed an additive effect. MST-312 is a synthetic compound derived from EGCG based on its telomerase inhibition activity and, there are currently no research looking into the effect of telomerase inhibitors in combination with quercetin. Because quercetin is a DNA intercalating agent that produces DNA damage and MST-312 induces telomeric damage owing to telomerase inhibition, we expected that their co-treatment would be extremely effective in reducing the cancer cell proliferation [15,21,22].

We investigated the effects of various dosages of quercetin and MST-312 on cell viability of ovarian cancer cells in the present study to establish their synergistic potential. We further studied the apoptosis, colony formation ability and DNA damage response induction upon co-treatment in cancer cells. As a control, we also investigated their effect on primary ovarian surface epithelial cells (OSEs).

Materials and methods

Reagents and cell culture

PA-1 (ovarian teratocarcinoma cell line), A2780 (ovarian adenocarcinoma cell line) A2780cisR (ovarian adenocarcinoma cisplatin-resistant cell line), OVCAR3 (ovarian adenocarcinoma cell line) and HCT116 (colorectal carcinoma) cells were cultured in Dulbecco's Modified Eagle Medium (DMEM) (High glucose with L-glutamine and sodium pyruvate) (HyClone, Cytiva, USA, Cat. No. SH30243.01) complemented with 10% heat inactivated fetal bovine serum (Gibco, ThermoFisher Scientific, USA, Cat. No. 10270106), 100 units/mL penicillin, 100 μg/mL streptomycin and 250 ng/mL amphotericin B (Gibco, Cat. No. 15240062) in a humidified 5% CO2 atmosphere at 37°C under standard cell culture conditions. All the cell lines were stained with Hoechst 33342, Trihydrochloride (Thermo Fischer) stain to check for mycoplasma. The cell lines were negative for mycoplasma. Human Ovarian Surface Epithelial (OSE) cells obtained from ScienCell Research Laboratories were cultured in Ovarian Epithelial Cell Medium (OEpiCM) (ScienCell Research Laboratories, USA, Cat. No. 7311) supplemented with 10% Ovarian Epithelial Cell Growth Supplement (OEpiCGS, ScienCell Research Laboratories Cat. No. 7352), 100 units/mL penicillin and 100 μg/mL streptomycin antibiotic solution (ScienCell Research Laboratories, Cat. No. 0503) under standard cell culture conditions.

Quercetin was obtained from Sigma-Aldrich (USA, Cat. No. Q4951) and its stock solution at concentration 100 mM was prepared fresh for every experiment, by dissolving it in dimethyl sulfoxide (DMSO). MST-312 (Cat. no. M3949) and luteolin (Cat. no. L9283) were purchased from Sigma-Aldrich Co. MST-312 was prepared in 20 mM stock solution and luteolin was prepared in 50 mM stock solution by dissolving them in DMSO. The stock concentrations of both were divided into aliquots and stored at -20°C until use.

Alamar blue cell viability assay

To study the effects of quercetin, MST-312 and luteolin independently on cell viability and logarithmic growth, PA-1, A2780 cells, OVCAR3, A2780cisR and HCT116 cells were seeded at a density of 8×104 cells/mL, 2×104 cells/mL, 9×104 cells/mL, 2×104 cells/mL and 1.5×104 cells/mL, respectively, in 96-well cell culture plates. Post 24 h, cells were incubated in the presence of increasing concentrations of quercetin and MST-312 for 72 h. Effect of luteolin on cell viability was evaluated in PA-1 cells for 72 h. Negative control (no compound) and vehicle control (DMSO) were maintained. After 72 h, cells were incubated in the presence of 20% solution (in DMEM) of 0.15 mg/mL alamar blue reagent in 1X Phosphate Buffered Saline (PBS) (pH 7.4) (Gibco, Cat. No.10010023) for 4 h at 37°C and absorbance was measured at 570 nm and 600 nm wavelengths in BioTek Epoch2 microplate reader (Agilent, USA) with Gen5 software (Version 3.03). OSE cells were seeded at a density of 4.5×10^4 cells/mL and the assay was performed as above. Percentage reduction of alamar blue reagent was calculated using the following formula;

$$\%\text{reductionofalamarblue} = \{[(O2xA1) - (O1xA2)] / [(R1xN2) - (R2xN1)]\}x100$$

Where:

O1 = Molar Extinction Coefficient of oxidized alamar blue at 570nm i.e. 80586
O2 = Molar Extinction Coefficient of oxidized alamar blue at 600nm i.e. 117216
R1 = Molar Extinction Coefficient of reduced alamar blue at 570nm i.e.155677
R2 = Molar Extinction Coefficient of reduced alamar blue at 600nm i.e. 14652
A1 = Absorbance value of test wells at 570nm
A2 = Absorbance value of test wells at 600nm
N1 = Absorbance value of negative control well at 570nm
N2 = Absorbance value of negative control well at 600nm

% reduction values were normalised to the control and then used to determine half-maximal inhibitory concentration (IC50) values from logarithmic growth curve using GraphPad Prism software (Version 8).

Determination of combination index and dose reduction index

To study the effects of combinatorial treatment of quercetin, MST-312 and Luteolin, above method for determination of cell viability using alamar blue was followed post incubation in the presence of various concentrations of quercetin and MST-312 or luteolin and MST-312 in combination for 72 h. Combination index (CI) was calculated using CompuSyn software according to the classic isobologram equation, $CI = D1/D_x1 + D2/D_x2$, where D_x1 and D_x2 indicate the individual doses of quercetin and MST-312 required to inhibit a given level of viability x and D1 and D2 indicate the doses of quercetin and MST-312 required to inhibit the same level of viability x in combination, respectively. CI values vary for each combination, as presented in the CI versus FA plot using MS Excel. Dose reduction Index (DRI) is the dose which may be reduced in a combination to produce effect x as opposed to the dose of individual compound alone and is calculated as DRI $1 = D_x1/D1$ and DRI $2 = D_x2/D2$.

Trypan blue exclusion assay

PA-1, A2780 and OVCAR3 cells were seeded at required densities in cell culture dishes. Cells were treated with MST-312 and/or quercetin, for 24 h or 48 h with DMSO as control. After treatment, cells were washed once with 1X PBS, trypsinzed, centrifuged and resuspended in 1X PBS. Cells were stained with Trypan Blue solution (0.4%) (Thermo Scientific, Cat. No. 15250061). Trypan blue negative and total cells were counted in a Neubauer hemocytometer and expressed as a percentage of viable cells normalised with vehicle-treated cells.

Clonogenic survival assay

To study the anti-proliferative effects of quercetin and MST-312, PA-1, A2780 and HCT116 cells were seeded at a density of 8×103 cells/well,1×103 cells/well, 1×103 cells/well respectively in 6-well culture plates. After formation of visible colonies in 5 days, cells were incubated with quercetin and MST-312, alone and in combination, with DMSO as control for 48 h (PA-1) or 96 h (A2780 and HCT116). Cells were then gently washed with 1X PBS once and stained with 0.05% (w/v) crystal violet solution for 2 h at room temperature followed by one wash with distilled water and the colonies were photographed. Quantification of colonies in terms of intensity of stained cells against the plate background was performed using ImageJ software and relative colony number was plotted (http://rsbweb.nih.gov/ij/).

Annexin-V-FITC/PI assay

Cells were seeded at a density of 6×10^5 cells in 60 mm cell culture dishes. After 24 h, cells were incubated in the presence of quercetin (10 μM) and/or MST-312 (1 μM) for 24 h with DMSO as control. Trypsinised cells were washed twice with 1X PBS and resuspended in 1X Binding buffer (BD Biosciences, USA, Cat no. 556547, 51-66121E). 2 μl of Annexin V-FITC (BD Biosciences, Cat no. 556547, 51-65874X) was added to 100 μl 1X Binding buffer containing cells and incubated for 15 min at room temperature in dark. Following the incubation, 2 μl PI (BD Biosciences, Cat no. 556547, 51-66211E) was added to the cells. The stained cell suspension was added to FACS tubes containing 400 μl 1X binding buffer and measured by BD FACS ARIA flow cytometer. The data was analyzed using BD FACSDiva (Becton Dickinson, NJ, USA) software. Annexin V-positive and PI-negative cells were considered to be in early apoptotic phase, Annexin V-negative and PI-positive cells were considered to be in necrosis phase, cells having positive staining for both Annexin-V and PI were considered to undergo late apoptosis and cells negative for Annexin V and PI were considered to be live cells. The percentage of apoptotic cells were calculated by determining the percentage of early apoptosis and late apoptosis cells.

Western blot analysis

Cells were seeded at a density of 1.2×10^6 cells in 100 mm culture dishes. After 24 h, cells were incubated with quercetin and MST-312, alone and in combination, with DMSO as control for 24 h following which they were washed once with 1X PBS (pH 7.4) and lysed in 0.25ml Totex lysis buffer (20 mM HEPES, pH 7.9, 0.35 M NaCl, 20% glycerol, 1% NP-40, 1 mM $MgCl_2$, 0.5 mM EDTA) supplemented with protease inhibitor cocktail (Roche Diagnostics, USA, Cat No. 11844600) and phosphatase inhibitor sodium orthovanadate (Sigma-Aldrich, Cat. No. S6508). Following 30 min incubation on ice, cell debris was pelleted down by centrifugation at 13,000 rpm for 15 min at 4°C and the supernatant transferred to a fresh 1.5 mL centrifuge tube. Protein estimation was done using 1X Bradford reagent (Sigma-Aldrich, Cat. No. 56916) at 595 nm using Lambda 25 UV/Vis spectrophotometer with UV WINLAB software (Version 2.85.04) (PerkinElmer, USA). Normalized protein samples were prepared in SDS-polyacrylamide gel electrophoresis (SDS-PAGE) loading buffer, run on Nu-PAGE® 4-12% Bis-Tris 1.5mm gel (ThermoFisher Scientific, Cat. No. NP0336BOX) in Xcell Surelock Mini-Cell Electrophoresis System (ThermoFisher Scientific, Cat. No. EI0001) and transferred onto Immun-Blot® PVDF membrane (Bio-Rad, USA, cat no. 1620177) using the Trans-Blot® SD semi-dry transfer cell (Bio-Rad, cat no. 1703940). After overnight blocking at 4°C with 5% Non-fat dried milk (NFDM) in 1X PBS, the membrane was exposed to respective primary antibodies in 5% NFDM for 1.5 h at room temperature. After washing with PBST (0.1% Tween-20 in 1X PBS), the membrane was labelled with secondary antibody for 1.5 h at room temperature followed by PBST washes. Primary antibodies used are as follows: mouse monoclonal anti-p53 (DO-1) from Santa Cruz Biotechnology, USA (Cat. No. sc-126), rabbit monoclonal anti-p21 (12D1) from Cell Signaling Technology, USA (Cat. No. 2947), mouse monoclonal anti-phospho-Histone H2A.X (Ser139) clone JBW301 from Sigma-Aldrich (Cat. No. 05-636), mouse monoclonal anti-β-Actin clone AC-74 from Sigma-Aldrich (Cat. No. A5316), rabbit polyclonal anti p-p53 (S15) from Cell Signaling Technology, USA (Cat. No. 9284T) and mouse monoclonal anti GAPDH (6C5) from Santa Cruz Biotechnology, USA (Cat no. SC- 32233). Secondary antibodies, anti-mouse IgG-HRP (Cat. No. sc-358914) and anti-rabbit IgG-HRP (Cat. No. sc-2004) were obtained from Santa Cruz Biotechnology. Protein bands were detected using SuperSignal™ West Femto Maximum Sensitivity Substrate (Cat. No. 34094), SuperSignal™ West Pico PLUS Chemiluminescent Substrate (Cat. No. 34577), SuperSignal™ West Atto Ultimate Sensitivity Chemiluminescent Substrate (Cat. No. A38555) from ThermoFisher Scientific, USA. The blots were visualised using Bio-Rad Molecular Imager® ChemiDoc XRS+ System with Image Lab™ Software by Bio-Rad (Cat no. 1708265). Densitometry analysis was achieved using ImageJ software (http://rsbweb.nih.gov/ij/). Uncropped western blot images are included as Supplementary Fig. 6.

Real time telomerase repeats amplification protocol (Q- TRAP)

To study the effects of quercetin and MST-312 on telomerase activity, PA-1 cells were seeded at a density of 6×105 cells/well in 6-well culture plates. After 24 h, cells were incubated in the presence of quercetin (10 μM) and/or MST-312 (1 μM) for 24 h with DMSO as control. Post treatment, the cells were trypsinized and the cell number was calculated using trypan blue. According to the cell number, the cell pellet was incubated with NP40 lysis buffer (10mM Tris HCl, pH 8, 1mM MgCl2, 1mM EDTA,1% v/v NP40, 0.25mM sodium deoxycholate, 10% v/v glycerol, 150 mM NaCl, 5mM 2-mercaptoethanol, 1X protease inhibitor cocktail) for 45 min on ice. After centrifugation at 13,000 rpm for 10 min at 4°C, the supernatant was collected and the extract for 10,000 cells was used for PCR. The PCR reaction consists of SYBR™ Green PCR Master Mix (ThermoFisher Scientific, Cat. No. 4344463), 10mM EGTA, 100 ng/ μl TS primer (5′ AAT CCG TCG AGC AGA GTT 3') and 100 ng/ μl ACX primer (5′ GCG CGG CTT ACC CTT ACC CTT ACC CTA ACC 3'). Using the StepOne™ Real-Time PCR System (ThermoFisher Scientific) samples were incubated for 30 min at 30°C followed by initial activation at 95°C for 10 min and amplification by 40 PCR cycles with 15 s at 95°C and 60 s at 60°C conditions. The threshold cycle values (Ct) were determined and telomerase activity was calculated using the following formula: relative telomerase activity (RTA) of sample = 10((Ct sample-Y-intercept)/slope). Y-intercept and slope were calculated from standard curve generated from serial dilutions of PA-1untreated cells (10000, 5000, 1000, 100 cells). RNase A (Thermo scientific, Cat. No. EN0531) treated sample was used as negative control and lysis buffer was used as no template control.

Immunofluorescence staining

PA-1 and A2780 cells were seeded on 2-well cell culture dishes at a density of 1×105 and 0.8×105 cells/well respectively. PA-1 cells were treated with quercetin (10 μM) and/or MST-312 (1 μM) for 24 h. A2780 cells were treated with quercetin (15 μM) and/or MST-312 (2 μM) for 48 h. The cells were washed with PBS three times, fixed with 4% paraformaldehyde for 15 min, and permeabilized in 0.2% Triton X-100 for 20 min. After blocking with 5% normal goat serum (Santa Cruz Biotechnology, USA, Cat no. sc-2043) for 1 h at room temperature, the cells were incubated with primary antibody, mouse monoclonal anti-phospho-Histone H2A.X (Ser139) clone JBW301 from Sigma-Aldrich (Cat. No. 05-636; 1:3500), overnight at 4°C. Goat anti-mouse IgG (H+L) highly cross-absorbed, Alexa FluorTM488 from Thermo Fischer (Cat. No. A11029; 1:2500) was used as a secondary antibody and incubated on the cells for 1 h in the dark at room temperature. The cells were washed with PBS and mounted with ProlongTM gold antifade

reagent with DAPI from Thermo Scientific (Cat. no. P36941). Images for PA-1 were acquired on a Vert. A1 Axio vision (Carl Zeiss) inverted fluorescence microscope at 40X magnification and for A2780 on Zeiss Axio-Observer Z1 microscope (LSM 780) at 63X magnification. For quantification of γ-H2AX foci, random fields of cells from each slide were quantified manually and calculated using the formula: Percentage of total γ-H2AX positive cells = (No. of cells containing ≥5 foci/ total number of cells) x 100.

Real-time PCR amplification

Cells were seeded at a density of 1.2×106 cells in 100 mm culture dishes. After 24 h, cells were incubated with quercetin and MST-312, alone and in combination, with DMSO as control for 24 h following which they were washed once with 1X PBS (pH 7.4) and total RNA was extracted using TRIzol™ Reagent (ThermoFisher Scientific, Cat. No. 15596018). Reverse transcription reaction was performed using Maxima First Strand cDNA Synthesis Kit (ThermoFisher Scientific, Cat. No. K1641). The synthesised cDNA was subjected to quantitative real time PCR using PowerUp™ SYBR™ Green Master Mix (ThermoFisher Scientific, Cat. No. A25741) in a StepOne™ Real-Time PCR System (ThermoFisher Scientific, Cat. No. 4376357). Thermal cycling conditions were as follows: Initial activation at 95°C for 3 min followed by 40 cycles of denaturation step at 94°C for 10 seconds and combined annealing/extension step at 62°C (p21)/ 60°C (ATM, RAD50 and GAPDH) for 30 seconds. A melt curve analysis was included to verify the specificity of primers and the relative quantification values were calculated using the 2-ΔΔCt relative expression formula. Nucleotide sequences of the primers used are: human p21 forward primer 5'-ACTGTCTTGTACCCTTGTGC-3' and reverse primer 5'-CCTCTTGGA-GAAGATCAGCC-3'; human GAPDH forward primer 5'-GTC AGT GGT GGA CCT GAC CT-3' and reverse primer 5'-CAC CAC CCT GTT GCT GTA GC-3'; human RAD50 forward primer 5'-CAT TCT GGG CGT GCG GAG-3' and reverse primer 5'-TCT TGA GCA ACC TTG GGA TCG TG-3'; human ATM forward primer 5'-CTC TGA GTG GCA GCT GGA AGA-3' and reverse primer 5'- TTT AGG CTG GGA TTG TTC GCT -3'. Each sample was analysed in duplicates for three data sets.

Statistical methods

We have employed one-way ANOVA (non-parametric analysis) with Dunnett's or Bonferroni's Multiple Comparison test unless specified in the legend. *P* value of <0.05 is considered statistically significant. Statistical analysis is performed using GraphPad Prism (version 8) software.

Results

Quercetin and MST-312 induce cytotoxicity in ovarian cancer cells

We treated PA-1, A2780, OVCAR3 and A2780$_{cisR}$ ovarian cancer cells and HCT116 colon cancer cells with increasing doses of quercetin (1–100 μM for PA-1 and 1–400 μM for A2780, OVCAR3, A2780$_{cisR}$ and HCT116) and MST-312 (0.01–50 μM) for 72 h and measured cell viability using the alamar blue assay. To determine whether the effects are unique to ovarian cancer or are similar in other cancer cells, HCT116 cells were included. Both quercetin and MST-312 induced cytotoxicity in the ovarian cancer cell lines and colon cancer cell line in a dose-dependent manner (Figs. 1 and supplementary 1A–D). IC_{50} for MST-312 in PA-1, A2780, OVCAR3, A2780$_{cisR}$ and HCT116 cell lines were 4.2 μM, 3.9 μM, 7.1 μM, 3.6 μM and 5.9 μM, respectively. For quercetin, IC_{50} were 12.9 μM, 55.4 μM, 216.2 μM, 112.2 μM and 227.6 μM for PA-1, A2780, OVCAR3, A2780$_{cisR}$ and HCT116 cell lines, respectively.

We further assessed the cytotoxic effect of quercetin and MST-312 in primary ovarian surface epithelial cells (OSEs) (Fig. 1D and H). IC_{50} for MST-312 in OSEs was 8 μM and for quercetin it was 17.5 μM (Fig. 1D and H). Bar graph representation of data from Fig. 1 (supplementary Fig. 1E–L) highlights the cytotoxicity concentration of compounds across cell lines. Comparing OSE cells to PA-1, A2780, and OVCAR3 cells, MST-312 was not cytotoxic at concentrations up to 5 μM, but quercetin displayed a comparable cytotoxicity range as observed with PA-1 cancer cells (Supplementary Fig. 1E–L). Notably, MST-312 showed a protective effect on OSEs at low concentrations.

Combination of quercetin and MST-312 shows synergistic cytotoxicity in ovarian cancer cells

To examine the effects of combinatorial treatment, we treated PA-1 cells with different concentrations of quercetin (5, 10 and 15 μM) and MST-312 (0.5, 1 and 2 μM), alone and in combination for 72 h. As shown in Fig. 2A and B, we observed that quercetin and MST-312 combination very significantly reduced cell viability of PA-1 cells as compared to both the compounds alone. Similarly, we treated A2780 cells with different concentrations of quercetin (15, 35 and 55 μM) and MST-312 (2, 3 and 4 μM) alone and in combination for 72 h. As shown in Fig. 2C and D, the combinatorial treatment led to significant increase in cytotoxicity as compared to individual compounds. Next, we treated OVCAR3 cells with different concentrations of quercetin (15, 30, 60 and 90 μM) and MST-312 (1 and 2 μM) alone and in combination for 72 h. As shown in Fig. 2E and F, the combinatorial treatment led to significant increase in cytotoxicity as compared to the compounds alone. A2780$_{cisR}$ and HCT116 cells also showed significantly increased cytotoxicity upon combinatorial treatment (Supplementary Fig. 2A–D). We also investigated the combination of MST-312 with quercetin in OSE cells and noted no significant effect in cell viability at the concentrations used (Fig. 2G and H).

Since cell viability in combination studies was measured using alamar blue absorbance assay, we also measured the cell viability changes by direct measurement of cell number using trypan blue exclusion method. We observed a significant reduction in the percentage of viable cells in the combination treated groups in PA-1, OVCAR3 and A2780 cells (Supplementary Fig. 2E–G).

Data from Fig. 2 and supplementary Fig. 2A–D was analysed in the CompuSyn software, which calculated the combination index (CI) to determine synergism (CI < 1), antagonism (CI > 1) or additive effect (CI = 1) of drug combinations. Software gave CI values of the combinations (Supplementary Table 1A). Isobologram analysis and Fraction affected (FA) versus CI plots were generated using the software and they revealed strong synergism for most of the doses in combination (Figs. 3; Supplementary 3A–D).

We further investigated whether luteolin, which is an analog of quercetin, could also synergize with MST-312 for inhibiting cancer cell proliferation. Dose-response curve for luteolin (range from 1 μM–256 μM) was generated in PA1 cells and IC_{50} of luteolin for PA1 was found to be 5.5 μM (Supplementary Fig. 4A). Combination of luteolin with MST-312 exhibited significantly increased cytotoxicity as compared to the compounds alone (Supplementary Fig. 4B–C). Analysis of the data from supplementary Fig. 4B–C in compusyn software suggested strong synergism for the combination (Supplementary Table 1B).

Thus, quercetin and MST-312 synergize to enhance cytotoxicity in PA-1, A2780, OVCAR3, A2780$_{cisR}$ and HCT116 cells. Analog of quercetin also synergizes with MST-312 to enhance the cytotoxicity in cancer cells.

Co-treatment with quercetin and MST-312 decreases colony formation and increases apoptosis in ovarian cancer cells

We further assessed the effect of quercetin, MST-312 and their combination on colony forming ability of PA-1, A2780 and HCT116 cells. Fig. 4A shows the images of the colonies obtained upon individual and combination treatment with quercetin and MST-312 and Fig. 4 B–D shows their quantification. Combination treatment significantly reduced the colony formation ability of PA-1, A2780 and HCT116 cells as

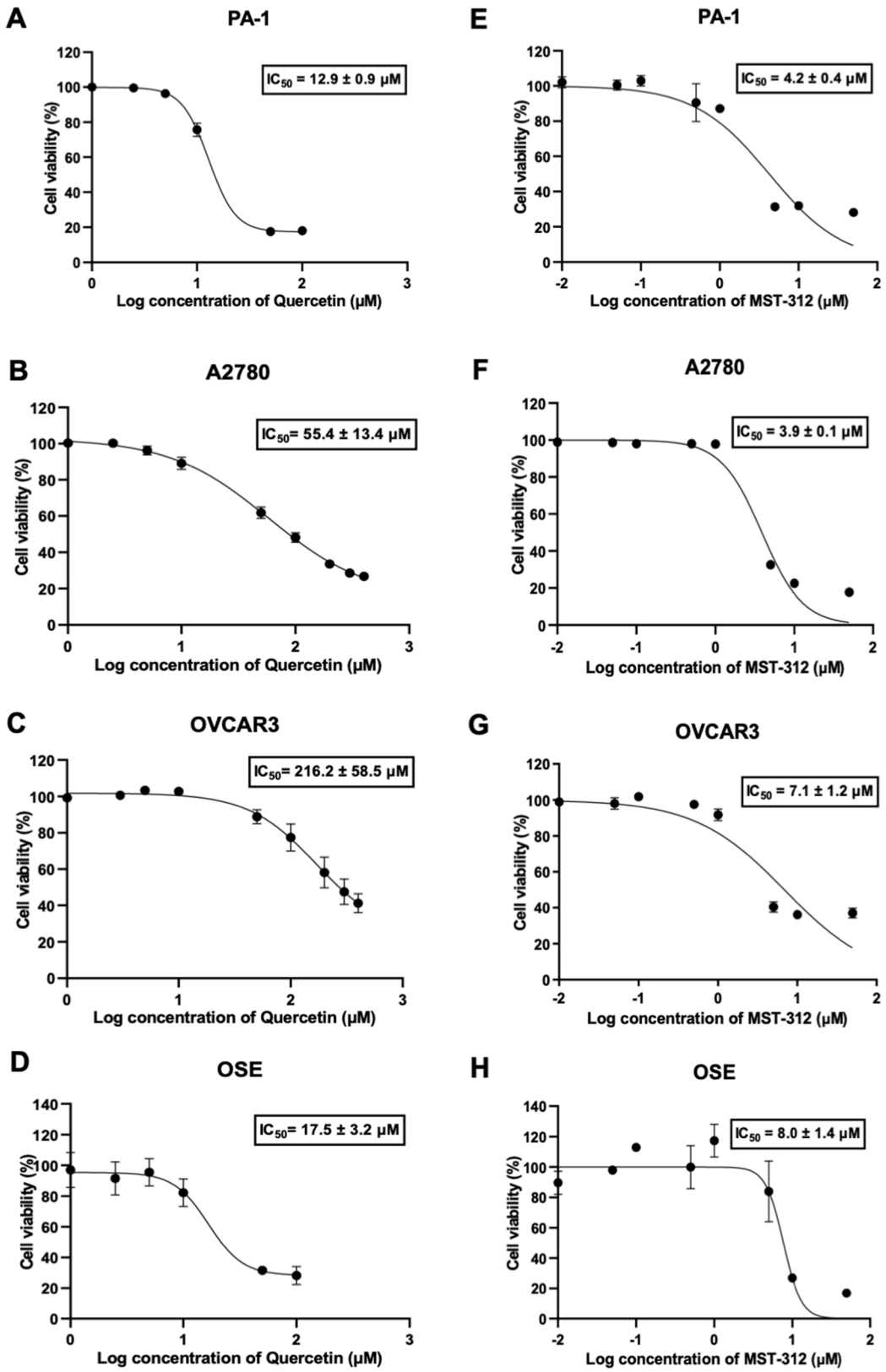

Fig. 1. Quercetin and MST-312 induce cytotoxicity in ovarian cancer cells. Cell viability after 72 h treatment with quercetin or MST-312 was determined by performing alamar blue assay and IC_{50} was calculated using Graphpad Prism software. DMSO treated cells served as vehicle control in all experiments. (A–D) Percentage cell viability of PA-1, A2780, OVCAR3 and OSE cells, respectively, after treatment with quercetin at various concentrations. (E–H) Percentage cell viability of PA-1, A2780, OVCAR3 and OSE cells, respectively, after treatment with MST-312 at various concentrations. Data represents mean ± SEM of three or more independent experiments for PA-1, A2780 and OVCAR3 cells and of two independent experiments for OSE cells.

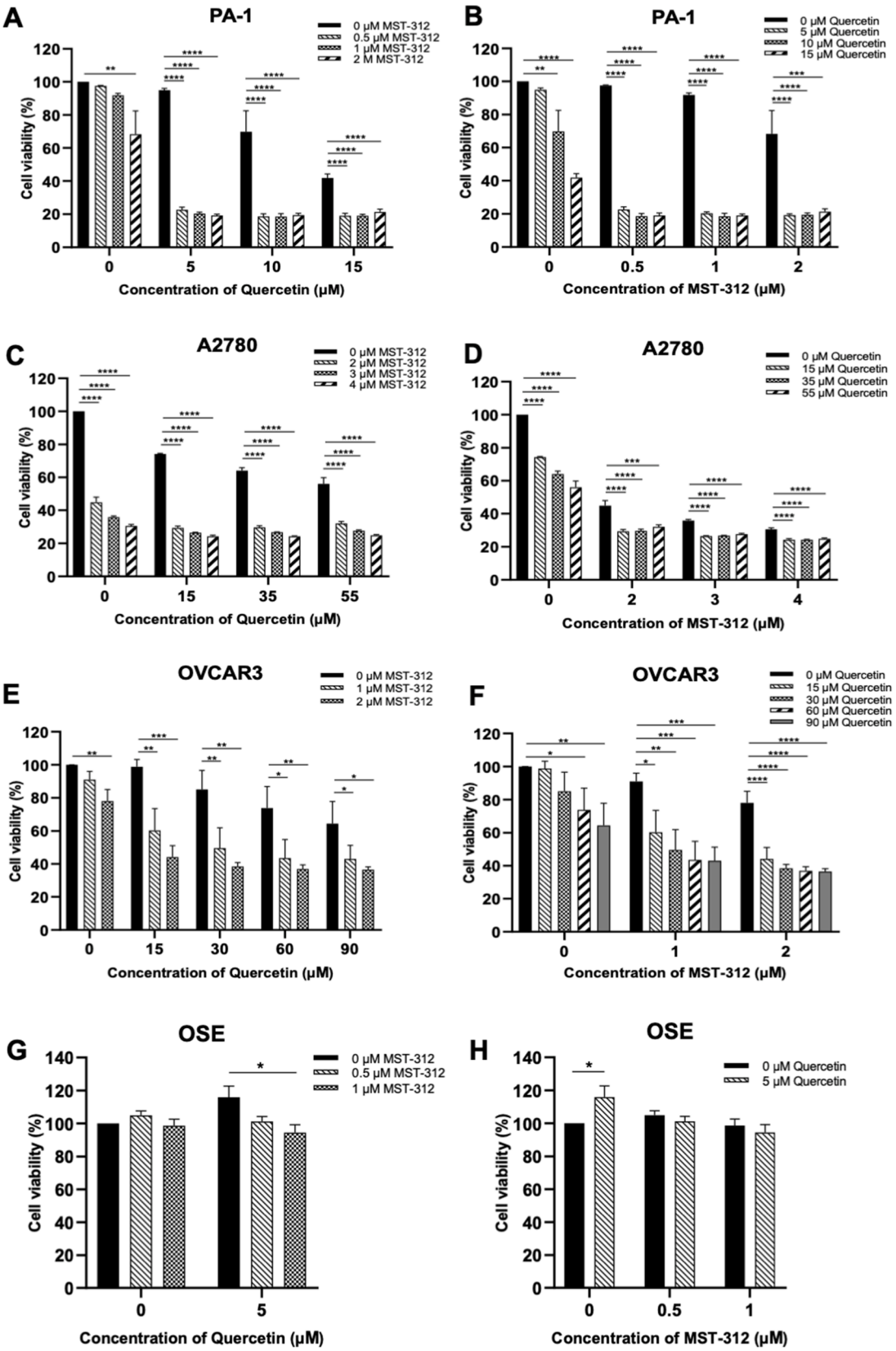

Fig. 2. Combinatorial effect of quercetin and MST-312 on PA-1, A2780, OVCAR3 and OSE cells. Following co-treatment with different concentrations of quercetin and MST-312, cell viability was determined using alamar blue assay. (A, B) Percentage cell viability after combination treatment with quercetin and MST-312 in PA-1 cells. (C, D) Percentage cell viability after combination treatment with quercetin and MST-312 in A2780 cells. (E, F) Percentage cell viability after combination treatment with quercetin and MST-312 in OVCAR3 cells. (G, H) Percentage cell viability after combination treatment with quercetin and MST-312 in OSE cells. Values represent mean ± SD of three independent experiments for PA-1, A2780 and OVCAR3 cell lines and of two independent experiments for OSE cell line, respectively, analysed by ANOVA with Dunnett's Multiple Comparison test. *$p \leq 0.05$; **$p \leq 0.01$; ***$p \leq 0.001$; ****$p \leq 0.0001$ represent significant changes.

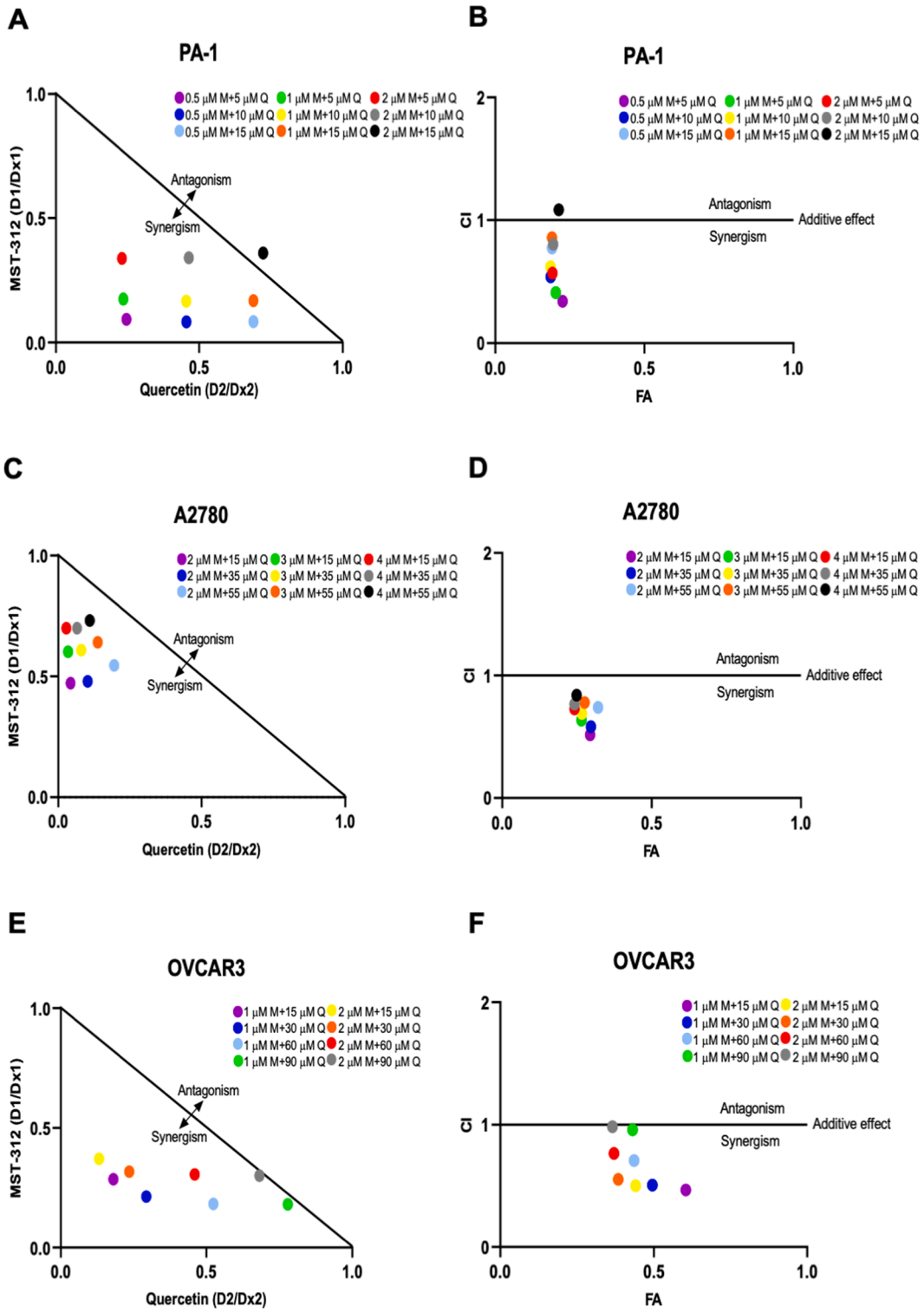

Fig. 3. Synergistic effect of quercetin and MST-312 in PA-1, A2780 and OVCAR3 cells. (A) Isobologram analysis of quercetin and MST-312 co-treatment in PA-1 cells was performed. CI values were calculated according to the classic isobologram equation (see materials and methods). D_x1 and D_x2 indicate the individual doses of quercetin and MST-312 required to inhibit a given level of viability x and D1 and D2 indicate the doses of quercetin and MST-312 required to inhibit the same level of viability x in combination, respectively. Points below the isoeffect line indicate synergism and those above the line indicate antagonism. (B) CI versus FA plot for the nine drug combinations of quercetin and MST-312 in PA-1 cells. (C, D) Isobologram analysis and CI versus FA plot for the nine drug combinations of quercetin and MST-312 in A2780 cells. (E-F) Isobologram analysis and CI versus FA plot for the eight drug combinations of quercetin and MST-312 in OVCAR3 cells. CI<1, =1 and >1 indicate synergism, additive effect and antagonism, respectively. Values are taken as the mean of three independent experiments.

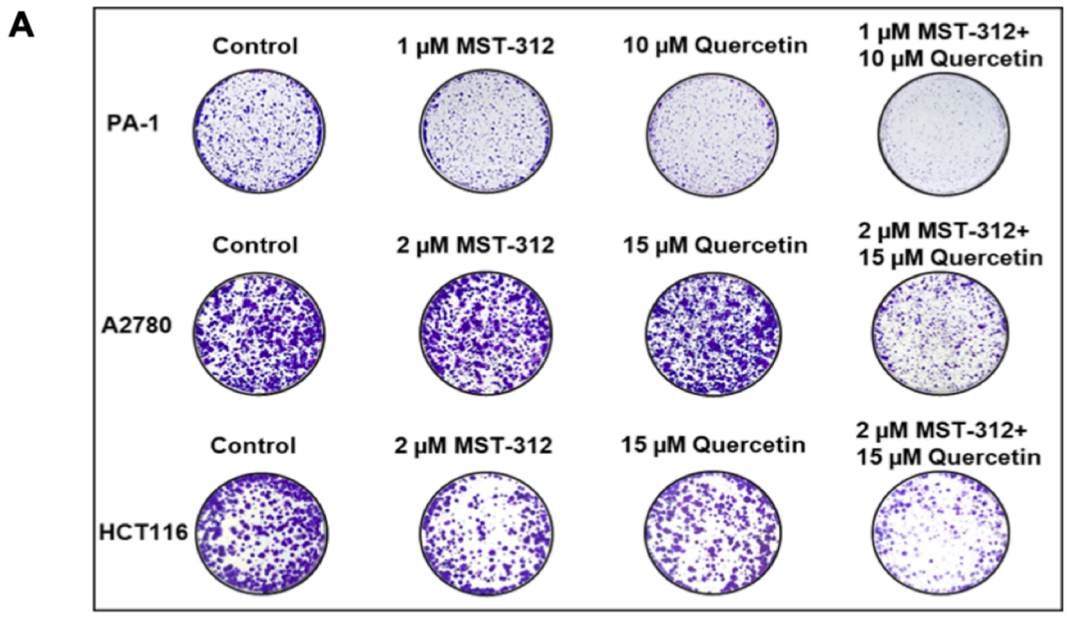

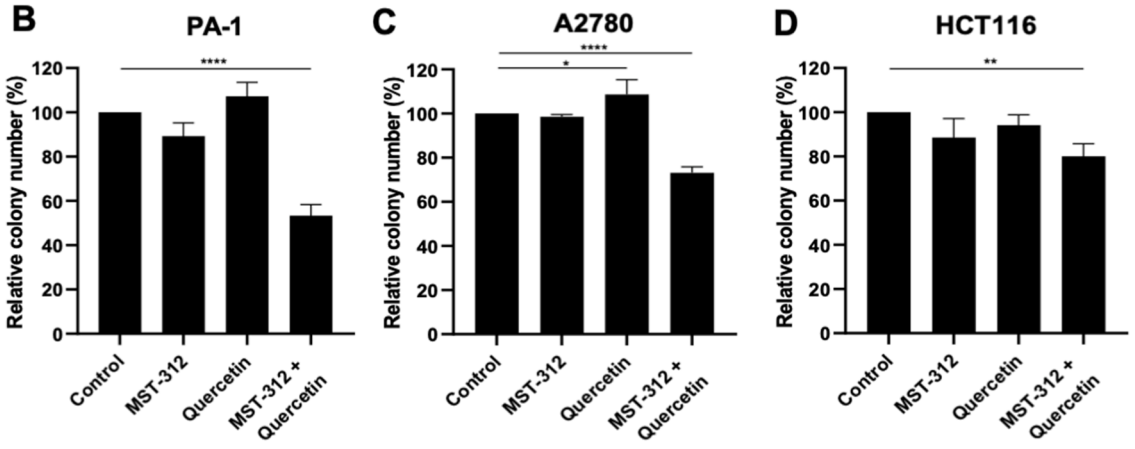

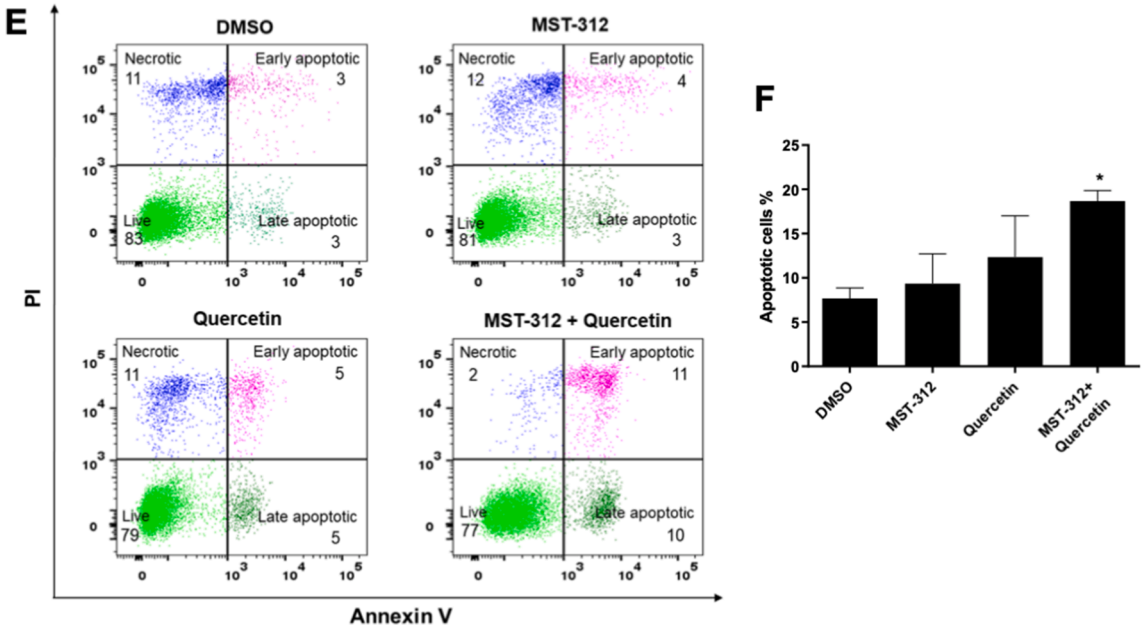

(caption on next page)

Fig. 4. Effect of quercetin and MST-312 on colony forming ability in PA-1, A2780 and HCT116 cells and on apoptosis in PA-1 cells. (A) Representative images from three technical replicates for clonogenic assay. PA-1 cells were treated with 1 μM MST-312 or 10 μM quercetin and their combination for 48 h, and A2780 and HCT116 cells were treated with 2 μM MST-312 or 15 μM quercetin and their combination for 96 h each. DMSO-treated cells were used as control. Colonies were stained with crystal violet solution and photographed. (B–D) Colonies were quantified using ImageJ software as colony number relative to control in PA-1, A2780 and HCT116 cells respectively. Values represent mean ± SD of three technical replicates analysed by ANOVA with Dunnett's Multiple Comparison test. *$p \leq 0.05$; **$p \leq 0.01$; ***$p \leq p \leq 0.001$; ****$p \leq 0.0001$ represent significant changes. (E) PA-1 cells were treated with 1 μM MST-312 and/or 10 μM Quercetin for 24 h and stained with Annexin V-FITC and PI, measured by BD FACS ARIA flow cytometer. Percentage of apoptotic cells were quantified using BD FACSDiva software. Scatter plots represent percent (%) of necrotic cells (upper left quadrant), late apoptotic cells (upper right quadrant), early apoptotic cells (lower right quadrant) and live cells (lower left quadrant). The data shown are representative of two independent experiments. (F) Each column represents mean ± SEM of values obtained from three independent experiments, analysed by two tailed paired student's t test (*$p \leq 0.05$).

compared to individual treatments thereby confirming that the combinatorial treatment of quercetin and MST-312 effectively exacerbates cell death in these cells.

Next, we assessed the apoptosis in PA-1 cells upon treatment with quercetin, MST-312 and their combination using Propidium Iodide and FITC Annexin V Apoptosis Detection Kit I. We found that combination treatment with MST-312 and quercetin significantly enhanced the proportion of apoptotic cells when compared to the control or single drug treatment groups (Fig. 4F). MST-312 and quercetin co-treatment induced 18.7 % apoptosis, which is higher than 9.3 % apoptosis caused by MST-312 or 12.3 % caused by quercetin alone.

Taken together, the above evidence implies that the combination of MST-312 and quercetin increases apoptosis and significantly impairs the colony formation ability of cancer cells.

Combination of quercetin and MST-312 augment DNA damage in cancer cells

PA-1 cells were treated with MST-312 and quercetin, alone and in combination. DMSO was used as a vehicle control and expression levels of DNA damage response protein p53, its downstream target, p21 and a biomarker for DNA damage, γ-H2AX, were measured using western blotting. 0.5 μM doxorubicin treated cells served as a positive control for the expression of DNA damage response proteins. A significant increase in the expression of p53, p21 and γ-H2AX was observed in combination-treated cells, when compared to the single compound treatment indicating that the combination induces increased DNA damage in PA-1 cells (Figs. 5A and Supplementary 5A). We did not observe any change in the protein expression of DNA damage response proteins upon MST-312 treatment alone when compared with vehicle control by western blotting. This could be because of low dosage of MST-312 and early time point of analysis which we selected, because upon increasing treatment time, cells in the combination treatment set underwent apoptosis limiting the amount of sample available for analysis. However, we measured the expression of p21 mRNA using real time PCR and observed a trend of increased expression upon MST-312 treatment compared to the vehicle control group (Supplementary Fig. 5B). Significant upregulation of p21 expression occurred upon co-treatment as is observed in real time PCR analysis and western blotting (Figs. 5A and Supplementary 5B).

Next we assessed the expression of γ-H2AX in A2780, OVCAR3 and OSEs upon treatment with MST-312 and quercetin, alone and in combination. We found increased expression of γ-H2AX in A2780 and OVCAR3 cells, while no γ-H2AX upregulation was observed in OSEs (Fig. 5B–C).

γ-H2AX accumulates at damaged DNA sites and appear as foci when observed microscopically using immunofluorescence (IF) assay. Therefore, we performed the IF analysis for γ-H2AX detection in PA1 and A2780 cells treated with quercetin and MST-312 alone and their combination. The co-treatment induced a significant increase in γ-H2AX foci in both cell lines (Supplementary Fig. 5C and E). In PA-1 cells, the percentage of γ-H2AX foci positive cells upon co-treatment was 33.3% which is higher than 15.97% by MST-312 and 24.01% by quercetin alone (Supplementary Fig. 5D). In A2780 cells, the percentage of γ-H2AX foci positive cells upon co-treatment was 47.63%, which is higher than 32.36% by MST-312, and 31.19% by quercetin alone (Supplementary Fig. 5F).

Additionally, we studied the effect of MST-312 and quercetin in PA-1 cells at different doses to determine the dose of each drug that exhibits a comparable cytotoxicity compared to the combination treatment. PA-1 cells were treated with different concentrations of MST-312 (1, 2, and 3 μM), quercetin (5, 10, and 20 μM) and the combination of MST-312 (1 μM) with quercetin (10 μM) for 24 h with DMSO as vehicle control. An increase in the expression of p53, p-p53 and γ-H2AX was observed with increasing concentrations of quercetin and MST-312 alone (Fig. 5D). The highest concentrations of MST-312 (3 μM) and quercetin (20 μM) showed elevated levels of p53 and p-p53 proteins similar or more than in the combination treated group when normalised to GAPDH. The highest concentration of quercetin (20 μM) showed higher levels of γ-H2AX than the combination treated group, confirming that low doses of quercetin (10 μM) and MST-312 (1 μM) in combination synergistically increase DNA damage.

We further wanted to understand the mechanism behind increased DNA damage upon combination treatment with MST-312 and quercetin. Both MST-312 and quercetin are known to inhibit telomerase activity and since inhibition of telomerase is known to cause telomere uncapping and increased DNA damage, we measured the telomerase activity in PA1 cells treated with quercetin and MST-312 alone and their combination. MST-312 treated cells did not show any change in telomerase activity as it is reported that MST-312 associates reversibly with telomerase and is washed off during dilution of cell lysate in assay buffer [16]. Quercetin treated cells displayed 100-fold reduction in telomerase activity when compared to vehicle control while cells treated with combination of MST-312 and quercetin displayed 1000-fold reduction in telomerase activity when compared to the vehicle control (Fig. 5E).

Additionally, MST-312 is reported to reduce the expression of homology repair pathway genes like ATM and RAD50 [15]. Therefore, we measured the gene expression of ATM and RAD50 in cells treated MST-312, quercetin and their combination. While we did not observe any change in ATM or RAD50 expression upon MST-312 treatment, we observed a significant reduction in the gene expression of ATM and RAD50 in the combination group compared to the vehicle control suggesting that damage induced in combination treated cells is not being repaired and thus gets accumulated and may contribute towards synergism (Fig. 5E).

Taken together, our findings demonstrate that co-treatment with MST-312 and quercetin augment DNA damage leading to increased cell death in cancer cells.

Discussion

The preclinical observations presented here have important implications in developing better cancer prevention and therapeutics. Our results demonstrate strong synergism between plant- derived flavonoid quercetin and telomerase inhibitor MST-312. We observed the synergism at the level of DNA damage induction, where co-treatment significantly upregulated the DNA damage response and apoptosis.

MST-312 displays two different types of effects on cancer cells. First, the acute cytotoxic effect, which occurs immediately post short-term treatment (72h) of MST-312. This is mostly attributed to the induction

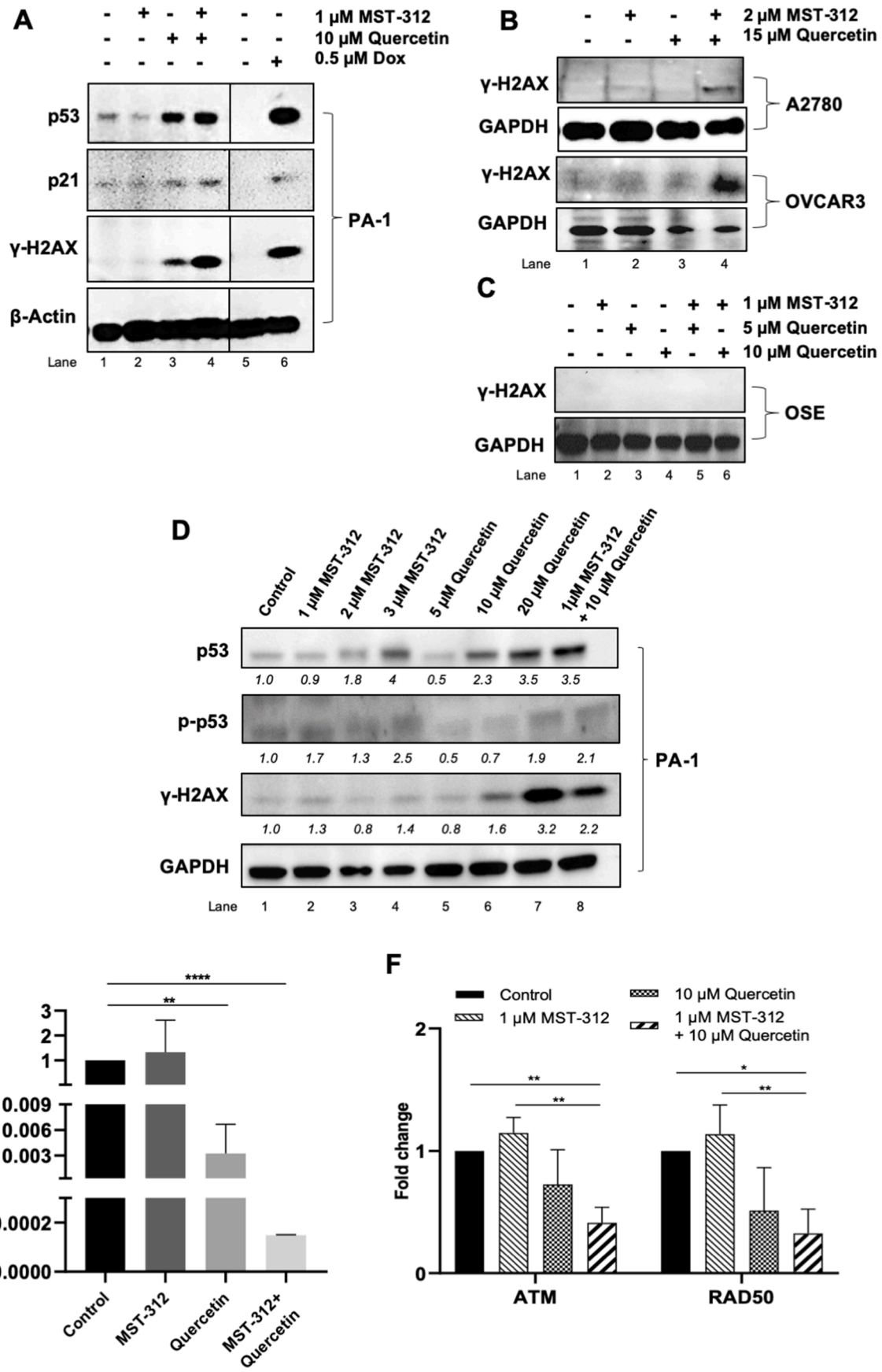

(caption on next page)

Fig. 5. Effect of quercetin and MST-312 on expression of DNA damage response proteins and telomerase activity. (A) PA-1 cells were treated with 1μM MST-312, 10 μM quercetin and their combination for 24 h. Control group was treated with DMSO as a vehicle. 0.5 μM Doxorubicin-treated cells served as positive control. Protein lysates were processed and analysed by Western blotting. β-Actin was used as the housekeeping protein. (B) A2780 and OVCAR3 cells were treated with 2μM MST-312, 15 μM quercetin and their combination for 48 h. Control group was treated with DMSO as a vehicle. (C) OSE cells were treated with 1μM MST-312, 5 μM or 10 μM quercetin and their combination for 24 h. (D) PA-1 cells were treated with different concentrations of MST-312 (1,2 and 3 μM) or quercetin (5,10 and 20 μM) and 1μM MST-312 + 10 μM quercetin for 24 h. Control group was treated with DMSO. Protein lysates were processed and analysed by Western blotting. GAPDH was used as the housekeeping protein. (E) Telomerase activity was measured in PA-1 cells subjected to MST-312 (1 μM) and/or quercetin (10 μM) treatment for 24 h by Q-TRAP assay. Samples were quantified as described in the protocol and plotted as RTA. RTA for an unknown sample was calculated based on standard curve and equation obtained from the same Q-TRAP assay using different cell numbers of PA-1 cells. Values represent mean ± SD of two independent experiments analysed by two tailed paired student's t test (**$p \leq 0.01$; ****$p \leq 0.0001$). (F) PA-1 cells were treated with 1μM MST-312, 10 μM quercetin and their combination for 24 h. Control group was treated with DMSO. Total RNA was extracted, reverse transcribed to cDNA and real-time quantitative PCR was performed. Total ATM and RAD50 gene expression was normalised to GAPDH. Data presented are mean ± SD from three biological repeats analysed by ANOVA with Bonferroni's Multiple Comparison test. (*$p \leq 0.05$; **$p \leq 0.01$).

of telomeric damage that occurs due to the inhibition of telomerase activity, which causes telomere uncapping followed by activation of DNA damage response and apoptosis or cell cycle arrest [15]. Second is the chronic effect, which occurs due to long-term continuous treatment with low concentration of MST-312, leading to telomere shortening and eventually resulting in replicative senescence [16]. Long-term treatment with MST-312 leads to resistance development in cancer cells by adapting alternative telomere lengthening mechanisms like selecting cells with long telomeres [23]. Thus, exploring the short-term chronic effect of MST-312 is therapeutically more viable prospect. Further, in the present study, we also monitored the acute cytotoxic effects in ovarian cancer cells. Notably, we also found that in normal OSE cells MST-312 was non-cytotoxic at doses up to 5μM (supplementary Fig. 1E–L). Interestingly, MST-312 was cytoprotective in OSEs at low concentrations and it would be interesting to explore the underlying mechanism for this observation.

Additionally, MST-312 specifically inhibits the telomerase activity at low concentrations (~1μM), while at high concentrations (~5μM) it inhibits DNA topoisomerase II. Telomerase inhibition results in telomere uncapping which leads to telomeric damage while DNA topoisomerase II inhibition results in general DNA damage. Thus, at lower concentrations, MST-312 induces telomeric DNA damage as is supported by detection of telomere induced foci (TIFs) formation while at higher concentrations it is capable of inducing telomeric as well as general DNA damage [15,16,24,25]. Interestingly, MST-312 is also reported to strongly bind with DNA as demonstrated using isothermal calorimetry analysis (ITC) assay and is suggested to competitively inhibit telomerase activity in brain tumor cell lines [26]. However, further experiments are required to determine whether MST-312 specifically associates with telomeric sequence or it has general affinity for the DNA double helix irrespective of the sequence or RNA-DNA hybrid formed during telomerase action. Further, the *in vivo* binding activity of MST-312 with DNA needs experimental confirmation. Quercetin binds to DNA via intercalation and causes double strand breaks thus affecting DNA metabolism [21]. Thus, there is a possibility that co-treatment with quercetin and MST-312 induces excessive DNA damage, which includes general as well as telomeric damage and that augments the apoptosis of cancer cells. However, both quercetin and MST-312 exhibit pleiotropic effects on cell signalling and synergy in modulating those activities cannot be overruled.

Additionally, we observed that homology repair pathway genes are significantly downregulated upon combined treatment with MST-312 and quercetin. Thus, there is possibility that damage by individual compounds is accumulating and instead of additive effect, the drug combination shows synergistic effect, where lower doses of drug combinations result in DNA damage levels which are otherwise achieved at very high concentrations, when used individually.

Quercetin acts as an anti-cancer chemo preventive and chemotherapeutic agent and its effects are reported for almost 20 different cancers using *in vitro* as well as *in vivo* assays (reviewed by Rauf et al) [7]. Treatment with quercetin shows a variety of effects in different cancer cells including inhibition of cell proliferation, inhibition of inflammation and reduction in invasion and metastasis by affecting multiple cell signalling pathways. Quercetin has poor pharmacological properties namely less absorption in gastrointestinal tract, huge first pass metabolism when consumed orally, instability in the gastrointestinal tract and poor solubility [27]. Phase I clinical trials with oral administration of quercetin have shown very variable results in terms of bioavailability mostly due to variations in quercetin-metabolizing enzymes and transporters [28]. Similarly, MST-312 also displays very low water solubility and unknown pharmacological properties. Thus, our study is significant in reporting that co-treatment with low doses of quercetin and MST-312 shows a strong synergistic effect in inhibiting cancer cell proliferation and causes enhanced DNA damage and apoptosis.

We further wanted to evaluate the importance of our proposed combination of compounds in comparison with reported combinations using these compounds in anti-cancer therapy. Thus, we collected the literature on various combinations of quercetin with chemotherapeutic drugs/compounds and MST-312 with chemotherapeutic drugs/compounds and tabulated (Table 1A, B). Interestingly, we observed that quercetin shows best synergism with DNA damaging chemotherapeutic agents. This is consistent with our observation, because MST-312 causes telomere dysfunction by activating DNA damage response that may synergize with the DNA damage response activation by quercetin. In addition, most of the combination studies with MST-312 do not report any combination index so it is difficult to understand the level of synergism.

Given the synergism observed by us in the current study, we also propose further investigations to explore the co-treatment as a cancer preventive and post-treatment supportive therapy to prevent cancer recurrence.

Supplementary Fig. 1. Quercetin and MST-312 induce cytotoxicity in ovarian cancer cell lines, OSE and HCT116. Cell viability after 72 h treatment with quercetin (5, 10 and 50 μM) or MST-312 (0.5, 1 2 and 5 μM) was determined by performing alamar blue assay using DMSO as vehicle control. (A-D) Percentage cell viability relative to untreated control in PA-1, A2780 OVCAR3 and OSE cells, respectively, treated with quercetin. (E-H) Percentage cell viability relative to untreated control in PA-1, A2780, OVCAR3 and OSE cells, respectively, treated with MST-312. Data represents mean ± SD of three or more independent for PA-1, A2780 and OVCAR3 and two independent experiments for OSE cells, respectively. (I-J) Percentage cell viability of A2780cisR and HCT116 cells, respectively, after treatment with quercetin at various concentrations. (K-L) Percentage cell viability of A2780cisR and HCT116 cells, respectively, after treatment with MST-312 at various concentrations. Data represents the mean ± SEM of three or more independent experiments. Data analysed by ANOVA with Dunnett's Multiple Comparison test. *$p \leq 0.05$; **$p \leq 0.01$; ***$p \leq 0.001$; ****$p \leq 0.0001$ represent significant changes.

Supplementary Fig. 2. Combinatorial effect of quercetin and MST-312 on ovarian and colorectal cancer cell lines. Following co-treatment with different concentrations of quercetin and MST-312, cell viability was determined using alamar blue assay. (A-B)

Table 1
Combinatorial treatments reported for quercetin with chemotherapeutic drugs/compounds in cancer cell lines.

A: Combination index for quercetin with chemotherapeutic drugs/compounds in cancer cell lines.

Sr. no.	Combination	Conc. of quercetin (μM)	Conc. of drug/ compound (μM)	Combination index (CI) reported	Cell line	Ref.
1	Quercetin and Cisplatin	7.5	10	0.34	Hela (cervical cancer)	[29]
		15		0.55		
		30		0.64		
		12.5	12	0.59	Siha (cervical cancer)	
		25		0.72		
		50		0.75		
	Quercetin and Cisplatin	5	80	1.11	C13* (ovarian cancer)	[30]
		10		1.28		
		15		1.21		
		20		1.16		
		30		1.15		
		40		0.97		
		60		0.96		
		80		0.97		
	Quercetin and Cisplatin	9.08–145.22	0.26–4.09	0.94	A2780 (ovarian cancer)	[31]
				0.88		
				0.72		
		10.38–166.10	1.66–26.52	0.4	A2780cisR (ovarian cancer)	
				0.46		
				0.27		
	Quercetin and Cisplatin	41.25–330	2.5–19.9	0.239 –0.474	HK1 (nasopharyngeal cancer)	[32]
		85–340	13–53	0.402–0.981	C666-1 (nasopharyngeal cancer)	
	Quercetin and Cisplatin	40	8.3	Not reported	HeP2 (laryngeal cancer)	[33]
	Quercetin and Cisplatin	50	10	Not reported	HepG2 (liver cancer)	[34]
2	Quercetin and Oxaplatin	9.08–145.22	0.16–2.62	0.91	A2780 (ovarian cancer)	[31]
				1.12		
				0.92		
		10.38–166.10	0.59–9.41	0.5	A2780cisR (ovarian cancer)	
				0.68		
				0.36		
3	Quercetin and Paclitaxel	7.5	0.01	2.69	HeLa (cervical cancer)	[29]
		15		1.63		
		30		1.39		
		12.5	0.006	1.71	SiHa (cervical cancer)	
		25		1.47		
		50		1.61		
	Quercetin and Paclitaxel	15	0.0125	0.55	PC-3 (prostate cancer)	[35]
	Quercetin and Paclitaxel	25	12.5	0.36	AGS-cyr61 (gastric cancer)	[36]
			25	1.86		
			50	6.87		
		50	12.5	0.73		
			25	0.51		
			50	0.48		
4	Quercetin and 5-Fluorouracil	7.5	6	2.6	HeLa (cervical cancer)	[29]
		15		1.15		
		30		1.19		
		12.5	50	1.15	SiHa (cervical cancer)	
		25		1.08		
		50		1.13		
	Quercetin and 5-Fluorouracil	25	6.25	0.33	AGS-cyr61 (gastric cancer)	[36]
			12.5	0.26		
			25	0.21		
		50	6.25	0.54		
			12.5	0.38		
			25	0.25		
	Quercetin and 5-Fluorouracil	50	100	Not reported	EC9706 and Eca109 (Esophageal cancer)	[37]
	Quercetin and 5-Fluorouracil	10	100	Not reported	HepG2 and SMCC-7721 (Liver cancer)	[38]
	Quercetin and 5-Fluorouracil	3.1–50	0.6	Not reported	HCT116 (Colon cancer)	[39]
5	Quercetin and Doxorubicin	7.5	0.075	1.48	HeLa (cervical cancer)	[29]
		15		1.23		
		30		1.32		
		7.5	0.1	1.01	SiHa (cervical cancer)	
		15		1.03		
		30		1.22		
	Quercetin and Doxorubicin	25	0.125	0.18	AGS-cyr61 (gastric cancer)	[36]
			0.25	0.2		
			0.5	0.2		
		50	0.125	0.34		

(*continued on next page*)

Table 1 (*continued*)

A: Combination index for quercetin with chemotherapeutic drugs/compounds in cancer cell lines.

Sr. no.	Combination	Conc. of quercetin (μM)	Conc. of drug/ compound (μM)	Combination index (CI) reported	Cell line	Ref.
			0.25	0.32		
			0.5	0.25		
	Quercetin and Doxorubicin	0.25–2	3.6	Not reported	MCF7 and MDA-MB-231 (Breast Cancer)	[40]
	Quercetin and Doxorubicin	5, 10	0.01, 0.1	Not reported	MCF7 and MDA-MB-231 (Breast Cancer)	[41]
6	Quercetin and Tamoxifen	25	3.125	0.89	AGS-cyr61 (gastric cancer)	[36]
			6.25	1.04		
			12.5	0.81		
		50	3.125	0.78		
			6.25	0.83		
			12.5	0.83		
7	Quercetin and Docetaxel	25	12.5	0.25	AGS-cyr61 (gastric cancer)	[36]
			25	1.2		
			50	2.96		
		50	12.5	0.81		
			25	1.2		
			50	0.59		
8	Quercetin and Bortezomib	20–60	0.02	Not reported	EBV transformed HRC57, DLBCL DoHH2 and U266 and RPMI-8226 (blood cancer)	[42]
9	Quercetin and Nocodazole	1–100	10	Not reported	HCT116 (Colon cancer)	[43]
10	Quercetin and Temozolomide	5, 15, 30	5–100	Not reported	MOGGCCM (Brain cancer)	[44]

B: Combinatorial treatments reported for MST-312 with chemotherapeutic drugs/compounds in cancer cell lines.

Sr. no.	Combination	Conc. of MST-312 (μM)	Conc. of drug/ compound (μM)	Combination index (CI) reported	Cell line	Ref.
1	MST-312 and Doxorubicin	2	10	1.16	NALM-6 (leukemia)	[45]
			20	0.68		
		4	10	0.79		
			20	1.19		
		2	5	0.84	REH (leukemia)	
			10	0.551		
		4	5	0.493		
			10	0.742		
2	MST-312 and 5-Flurouracil	3	0–50	Not reported	5-FU resistant HT-29 and SW620 (colon cancer)	[46]
3	MST-312 and NU7026	1	10	Not reported	MO59K (brain cancer)	[26]
4	MST and Docetaxel	2	3.9–250	Not reported	MDA-MB-231 cells (breast cancer)	[23]
5	MST and Irinotecan	2	3.9-250	Not reported	MDA-MB-231 cells (breast cancer)	

Percentage cell viability after combination treatment with quercetin and MST-312 in A2780cisR cells. (C-D) Percentage cell viability after combination treatment with quercetin and MST-312 in HCT116 cells. Values represent mean ± SD of three independent experiments analysed by ANOVA with Dunnett's Multiple Comparison test. *$p \leq 0.05$; **$p \leq 0.01$; ***$p \leq 0.001$; ****$p \leq 0.0001$ represent significant changes. (E) Percentage of viable PA-1 cells after treatment with 1μM MST-312 and/or 10 μM quercetin for 24 h was calculated using trypan blue exclusion method. (F) Percentage of viable A2780 cells after treatment with 2 μM MST-312 and/or 15 μM quercetin for 48 h was calculated using trypan blue exclusion method. (G) Percentage of viable OVCAR3 cells after treatment with 2 μM MST-312 and/or 15 μM quercetin for 48 h was calculated using trypan blue exclusion method. Percentage of viable cells in treated groups is normalised to that in control. Values represent mean ± SD of three independent experiments for PA-1 and OVCAR3 cell lines and of two independent experiments for A2780 cells, respectively, analysed by ANOVA with Dunnett's Multiple Comparison test. *$p \leq 0.05$; **$p \leq 0.01$; ***$p \leq 0.001$; ****$p \leq 0.0001$ represent significant changes.

Supplementary Fig. 3. Synergistic effect of quercetin and MST-312 in A2780cisR and HCT116 cells. (A) Isobologram analysis of quercetin and MST-312 co-treatment in A2780cisR cells was performed. CI values were calculated according to the classic isobologram equation (see materials and methods). Dx1 and Dx2 indicate the individual doses of quercetin and MST-312 required to inhibit a given level of viability x and D1 and D2 indicate the doses of quercetin and MST-312 required to inhibit the same level of viability x in combination, respectively. Points below the isoeffect line indicate synergism and those above the line indicate antagonism. (B) CI versus FA plot for the nine drug combinations of quercetin and MST-312 in A2780cisR cells. (C-D) Isobologram analysis and CI versus FA plot for the eight drug combinations of quercetin and MST-312 in HCT116 cells. CI<1, =1 and >1 indicate synergism, additive effect and antagonism, respectively. Values are taken as the mean of three independent experiments.

Supplementary Fig. 4. Combinatorial effect of luteolin and MST-312 on ovarian cancer cell line. Cell viability after 72 h treatment with luteolin was determined by performing alamar blue assay and IC50 was calculated using Graphpad Prism software. DMSO treated cells served as vehicle control in all experiments. (A) Percentage cell viability of PA-1 cells, after treatment with luteolin at various concentrations. (B-C) Following co-treatment with different concentrations of luteolin and MST-312, percentage cell viability was determined using alamar blue assay in PA-1 cells. Values represent mean ± SEM of two independent experiments analysed by ANOVA with Dunnett's Multiple Comparison test. *$p \leq 0.05$; **$p \leq 0.01$; represent significant changes.

Supplementary Fig. 5. Combined treatment with MST-312 and quercetin augment DNA damage in cancer cells. (A) Densitometric analysis of p53, p21 and γ-H2AX expression in PA-1 cells normalised to β-Actin. Data presented are mean ± SEM from three biological repeats analysed by ANOVA with Bonferroni's Multiple Comparison test. *$p \leq 0.05$; **$p \leq 0.01$; ****$p \leq 0.0001$ represent significant changes. (B) PA-1 cells were treated with 1μM MST-312, 10 μM quercetin and their

combination for 24 h. Control group was treated with DMSO. Total RNA was extracted, reverse transcribed to cDNA and real-time quantitative PCR was performed. p21 gene expression was normalised to GAPDH. Data presented are mean ± SD from three biological repeats analysed by ANOVA with Bonferroni's Multiple Comparison test. (**$p \leq 0.01$). Immunofluorescence detection of γ-H2AX foci in PA-1 and A2780 cells. (C) Representative fluorescence microscopy images of PA-1 cells treated with 1 μM MST-312 or 10 μM quercetin and their combination for 24 h. (D) Quantification of γ-H2AX foci positive cells in PA-1 cells. Scale bar indicate 50 μm. Data represents mean ± SD of two independent experiments analysed by ANOVA with Dunnett's Multiple Comparison test (*$p \leq 0.05$). (E) Representative fluorescence microscopy images of A2780 cells treated with 2 μM MST-312 or 15 μM quercetin and their combination for 48 h. (F) Quantification of γ-H2AX foci positive cells in A2780 cells. Data represents values from one experiment for A2780. Scale bars indicate 10 μm.

Supplementary Fig. 6. Uncropped images for Western blot analysis. (A) Uncropped image for Fig. 5A. (B) Uncropped image for Fig. 5B. (C) Uncropped image for Fig. 5C. (D) Uncropped image for Fig. 5D.

CRediT authorship contribution statement

Stina George Fernandes: Data curation, Writing – review & editing. **Kavita Gala:** Data curation, Writing – review & editing. **Ekta Khattar:** Data curation, Writing – review & editing, Funding acquisition.

Declaration of Competing Interest

The authors declare that they have no known competing financial interests or personal relationships that could have appeared to influence the work reported in this paper.

Funding and acknowledgments

EK is supported by a research grant from the Department of Biotechnology (No. BT/RLF/Re-entry/06/2015), Department of Science and Technology (ECR/2018/002117) and NMIMS Seed Grant (IO 401405). The authors would like to acknowledge FACS Central facility for flow cytometry data and Confocal Laser Scanning Microscope Facility for immunofluorescence data, IRCC, IIT Bombay.

Supplementary materials

Supplementary material associated with this article can be found, in the online version, at doi:10.1016/j.tranon.2022.101569.

References

[1] P. Gaona-Luviano, L.A. Medina-Gaona, K. Magaña-Pérez, Epidemiology of ovarian cancer, Chin. Clin. Oncol. 9 (4) (2020) 47.
[2] H. Sung, J. Ferlay, R.L. Siegel, M. Laversanne, I. Soerjomataram, A. Jemal, F. Bray, Global cancer statistics 2020: GLOBOCAN estimates of incidence and mortality worldwide for 36 cancers in 185 countries, CA Cancer J. Clin. 71 (3) (2021) 209–249.
[3] G.H. Giornelli, Management of relapsed ovarian cancer: a review, Springerplus 5 (1) (2016) 1197.
[4] P. Garcia-Oliveira, P. Otero, A.G. Pereira, F. Chamorro, M. Carpena, J. Echave, M. Fraga-Corral, J. Simal-Gandara, M.A. Prieto, Status and challenges of plant-anticancer compounds in cancer treatment, Pharmaceuticals 14 (2) (2021) (Basel).
[5] Y. Li, J. Yao, C. Han, J. Yang, M.T. Chaudhry, S. Wang, H. Liu, Y. Yin, Quercetin inflammation and immunity, Nutrients 8 (3) (2016) 167.
[6] C.G. Heijnen, G.R. Haenen, R.M. Oostveen, E.M. Stalpers, A. Bast, Protection of flavonoids against lipid peroxidation: the structure activity relationship revisited, Free Radic. Res. 36 (5) (2002) 575–581.
[7] A. Rauf, M. Imran, I.A. Khan, M. Ur-Rehman, S.A. Gilani, Z. Mehmood, M. S. Mubarak, Anticancer potential of quercetin: a comprehensive review, Phytother. Res. 32 (11) (2018) 2109–2130.
[8] A. Vafadar, Z. Shabaninejad, A. Movahedpour, F. Fallahi, M. Taghavipour, Y. Ghasemi, M. Akbari, A. Shafiee, S. Hajighadimi, S. Moradizarmehri, E. Razi, A. Savardashtaki, H. Mirzaei, Quercetin and cancer: new insights into its therapeutic effects on ovarian cancer cells, Cell Biosci. 10 (2020) 32.
[9] A. Murakami, H. Ashida, J. Terao, Multitargeted cancer prevention by quercetin, Cancer Lett. 269 (2) (2008) 315–325.
[10] K. Bishayee, A.R. Khuda-Bukhsh, S.O. Huh, PLGA-Loaded gold-nanoparticles precipitated with quercetin downregulate HDAC-Akt activities controlling proliferation and activate p53-ROS Crosstalk to induce apoptosis in hepatocarcinoma cells, Mol. Cells 38 (6) (2015) 518–527.
[11] R. Aalinkeel, B. Bindukumar, J.L. Reynolds, D.E. Sykes, S.D. Mahajan, K.C. Chadha, S.A. Schwartz, The dietary bioflavonoid, quercetin, selectively induces apoptosis of prostate cancer cells by down-regulating the expression of heat shock protein 90, Prostate 68 (16) (2008) 1773–1789.
[12] R. Jagadeeswaran, C. Thirunavukkarasu, P. Gunasekaran, N. Ramamurty, D. Sakthisekaran, *In vitro* studies on the selective cytotoxic effect of crocetin and quercetin, Fitoterapia 71 (4) (2000) 395–399.
[13] J.H. Jeong, J.Y. An, Y.T. Kwon, J.G. Rhee, Y.J. Lee, Effects of low dose quercetin: cancer cell-specific inhibition of cell cycle progression, J. Cell. Biochem. 106 (1) (2009) 73–82.
[14] A.F. Brito, M. Ribeiro, A.M. Abrantes, A.S. Pires, R.J. Teixo, J.G. Tralhão, M. F. Botelho, Quercetin in cancer treatment, alone or in combination with conventional therapeutics? Curr. Med. Chem. 22 (26) (2015) 3025–3039.
[15] R.L. Gurung, S.N. Lim, G.K. Low, M.P. Hande, MST-312 alters telomere dynamics, gene expression profiles and growth in human breast cancer cells, J. Nutr. Nutr. 7 (4-6) (2014) 283–298.
[16] H. Seimiya, T. Oh-hara, T. Suzuki, I. Naasani, T. Shimazaki, K. Tsuchiya, T. Tsuruo, Telomere shortening and growth inhibition of human cancer cells by novel synthetic telomerase inhibitors MST-312, MST-295, and MST-1991, Mol. Cancer Ther. 1 (9) (2002) 657–665.
[17] Z. Ameri, S. Ghiasi, A. Farsinejad, G. Hassanshahi, M. Ehsan, A. Fatemi, Telomerase inhibitor MST-312 induces apoptosis of multiple myeloma cells and down-regulation of anti-apoptotic, proliferative and inflammatory genes, Life Sci. 228 (2019) 66–71.
[18] A. Fatemi, M. Safa, A. Kazemi, MST-312 induces G2/M cell cycle arrest and apoptosis in APL cells through inhibition of telomerase activity and suppression of NF-κB pathway, Tumour Biol. 36 (11) (2015) 8425–8437.
[19] P. Wang, D. Heber, S.M. Henning, Quercetin increased the antiproliferative activity of green tea polyphenol (-)-epigallocatechin gallate in prostate cancer cells, Nutr. Cancer 64 (4) (2012) 580–587.
[20] P. Wang, J.V. Vadgama, J.W. Said, C.E. Magyar, N. Doan, D. Heber, S.M. Henning, Enhanced inhibition of prostate cancer xenograft tumor growth by combining quercetin and green tea, J. Nutr. Biochem. 25 (1) (2014) 73–80.
[21] S. Srivastava, R.R. Somasagara, M. Hegde, M. Nishana, S.K. Tadi, M. Srivastava, B. Choudhary, S.C. Raghavan, Quercetin, a natural flavonoid interacts with DNA, arrests cell cycle and causes tumor regression by activating mitochondrial pathway of apoptosis, Sci. Rep. 6 (2016) 24049.
[22] A. Das, D. Majumder, C. Saha, Correlation of binding efficacies of DNA to flavonoids and their induced cellular damage, J. Photochem. Photobiol. B 170 (2017) 256–262.
[23] K.D.S. Morais, D.D.S. Arcanjo, G.P. de Faria Lopes, G.G. da Silva, T.H.A. da Mota, T.R. Gabriel, D.D.A. Rabello Ramos, F.P. Silva, D.M. de Oliveira, Long-term *in vitro* treatment with telomerase inhibitor MST-312 induces resistance by selecting long telomeres cells, Cell Biochem. Funct. 37 (4) (2019) 273–280.
[24] H. Takai, A. Smogorzewska, T. de Lange, DNA damage foci at dysfunctional telomeres, Curr. Biol. 13 (17) (2003) 1549–1556.
[25] C. Fujiwara, Y. Muramatsu, M. Nishii, K. Tokunaka, H. Tahara, M. Ueno, T. Yamori, Y. Sugimoto, H. Seimiya, Cell-based chemical fingerprinting identifies telomeres and lamin A as modifiers of DNA damage response in cancer cells, Sci. Rep. 8 (1) (2018) 14827.
[26] R.L. Gurung, H.K. Lim, S. Venkatesan, P.S. Lee, M.P. Hande, Targeting DNA-PKcs and telomerase in brain tumour cells, Mol. Cancer 13 (2014) 232.
[27] A.A. Date, M.S. Nagarsenker, S. Patere, V. Dhawan, R.P. Gude, P.A. Hassan, V. Aswal, F. Steiniger, J. Thamm, A. Fahr, Lecithin-based novel cationic nanocarriers (Leciplex) II: improving therapeutic efficacy of quercetin on oral administration, Mol. Pharm. 8 (3) (2011) 716–726.
[28] J.H. Moon, R. Nakata, S. Oshima, T. Inakuma, J. Terao, Accumulation of quercetin conjugates in blood plasma after the short-term ingestion of onion by women, Am. J. Physiol. Regul. Integr. Comp. Physiol. 279 (2) (2000) R461–R467.
[29] W. Xu, S. Xie, X. Chen, S. Pan, H. Qian, X. Zhu, Effects of quercetin on the efficacy of various chemotherapeutic drugs in cervical cancer cells, Drug Des. Dev. Ther. 15 (2021) 577–588.
[30] N. Li, C. Sun, B. Zhou, H. Xing, D. Ma, G. Chen, D. Weng, Low concentration of quercetin antagonizes the cytotoxic effects of anti-neoplastic drugs in ovarian cancer, PLoS One 9 (7) (2014), e100314.
[31] M.U. Nessa, P. Beale, C. Chan, J.Q. Yu, F. Huq, Synergism from combinations of cisplatin and oxaliplatin with quercetin and thymoquinone in human ovarian tumour models, Anticancer Res. 31 (11) (2011) 3789–3797.
[32] M. Daker, M. Ahmad, A.S. Khoo, Quercetin-induced inhibition and synergistic activity with cisplatin - a chemotherapeutic strategy for nasopharyngeal carcinoma cells, Cancer Cell Int. 12 (1) (2012) 34.
[33] H. Sharma, S. Sen, N. Singh, Molecular pathways in the chemosensitization of cisplatin by quercetin in human head and neck cancer, Cancer Biol. Ther. 4 (9) (2005) 949–955.
[34] J.L. Zhao, J. Zhao, H.J. Jiao, Synergistic growth-suppressive effects of quercetin and cisplatin on HepG2 human hepatocellular carcinoma cells, Appl. Biochem. Biotechnol. 172 (2) (2014) 784–791.
[35] X. Zhang, J. Huang, C. Yu, L. Xiang, L. Li, D. Shi, F. Lin, Quercetin enhanced paclitaxel therapeutic effects towards PC-3 prostate cancer through ER stress induction and ROS production, Onco Targets Ther. 13 (2020) 513–523.

[36] H.B. Hyun, J.Y. Moon, S.K. Cho, Quercetin suppresses CYR61-mediated multidrug resistance in human gastric adenocarcinoma AGS cells, Molecules 23 (2) (2018).
[37] L. Chuang-Xin, W. Wen-Yu, C. Yao, L. Xiao-Yan, Z. Yun, Quercetin enhances the effects of 5-fluorouracil-mediated growth inhibition and apoptosis of esophageal cancer cells by inhibiting NF-κB, Oncol. Lett. 4 (4) (2012) 775–778.
[38] W. Dai, Q. Gao, J. Qiu, J. Yuan, G. Wu, G. Shen, Quercetin induces apoptosis and enhances 5-FU therapeutic efficacy in hepatocellular carcinoma, Tumour Biol. 37 (5) (2016) 6307–6313.
[39] T. Samuel, K. Fadlalla, L. Mosley, V. Katkoori, T. Turner, U. Manne, Dual-mode interaction between quercetin and DNA-damaging drugs in cancer cells, Anticancer Res. 32 (1) (2012) 61–71.
[40] S. Li, S. Yuan, Q. Zhao, B. Wang, X. Wang, K. Li, Quercetin enhances chemotherapeutic effect of doxorubicin against human breast cancer cells while reducing toxic side effects of it, Biomed. Pharmacother. 100 (2018) 441–447.
[41] D. Staedler, E. Idrizi, B.H. Kenzaoui, L. Juillerat-Jeanneret, Drug combinations with quercetin: doxorubicin plus quercetin in human breast cancer cells, Cancer Chemother. Pharmacol. 68 (5) (2011) 1161–1172.
[42] F.T. Liu, S.G. Agrawal, Z. Movasaghi, P.B. Wyatt, I.U. Rehman, J.G. Gribben, A. C. Newland, L. Jia, Dietary flavonoids inhibit the anticancer effects of the proteasome inhibitor bortezomib, Blood 112 (9) (2008) 3835–3846.
[43] T. Samuel, K. Fadlalla, T. Turner, T.E. Yehualaeshet, The flavonoid quercetin transiently inhibits the activity of taxol and nocodazole through interference with the cell cycle, Nutr. Cancer 62 (8) (2010) 1025–1035.
[44] J. Jakubowicz-Gil, E. Langner, W. Rzeski, Kinetic studies of the effects of Temodal and quercetin on astrocytoma cells, Pharmacol. Rep. 63 (2) (2011) 403–416.
[45] N. Ghasemimehr, A. Farsinejad, R. Mirzaee Khalilabadi, Z. Yazdani, A. Fatemi, The telomerase inhibitor MST-312 synergistically enhances the apoptotic effect of doxorubicin in pre-B acute lymphoblastic leukemia cells, Biomed. Pharmacother. 106 (2018) 1742–1750.
[46] S.S. Chung, B. Oliva, S. Dwabe, J.V. Vadgama, Combination treatment with flavonoid morin and telomerase inhibitor MST-312 reduces cancer stem cell traits by targeting STAT3 and telomerase, Int. J. Oncol. 49 (2) (2016) 487–498.